Zeitschrift: Helvetica Physica Acta
Band: 48 (1975)
Heft: 4

Artikel: On the anomalous skin effect in metals. part 1, Normal conductors
Autor: Drangeid, K.E. / Sommerhalder, R.
DOI: https://doi.org/10.5169/seals-114682

Helvetica Physica Acta
Vol. 48, 1975.

Birkhäuser Verlag Basel

On the Anomalous Skin Effect in Metals
Part 1: Normal Conductors

by **K. E. Drangeid** and **R. Sommerhalder**

IBM Zurich Research Laboratory, 8803 Rüschlikon, Switzerland

(23. IV. 75)

Abstract. A study of an analog network model is presented which results in finding a set of differential equations describing transport phenomena in metals such as: a) dc size effects in thin films; b) ac impedance of bulk material in the microwave range; c) bulk absorption up to the optical range, in terms of coupled ordinary waves. Solutions are in very close agreement with experimental evidence.

The model further generates an expression for the reciprocal surface impedance which is well suited as a response function in connection with the Kramers–Kronig relations.

1. Introduction

The phenomenon of the anomalous skin effect in metals was first explained by Pippard [1] and Reuter and Sondheimer [2] in terms of single-particle electron theory. Because their results were so nicely in agreement with known phenomenology, and evolved from the general methods of the theory of metals, the Reuter–Sondheimer theory soon became – and still is – widely used. The physical picture of current transport involved with it permits, in an unbounded metal, ordinary wave propagation when the mean free path of the conduction electrons is small, but not when the free path becomes larger than some critical value (Pippard, Reuter and Sondheimer [3], see also Serin [4]). In the former case, there is a correspondence between electric field and current density in a bounded metal which is not affected by the presence of the surface, while in the latter case current excitation is conditioned at all points of the metal by the presence of the surface. In other words, a metal shows regular impedance behavior when the mean free path of the conduction electrons is small, but loses this property when the free path becomes too large.

In this paper, an unconventional approach for a many-body standpoint is made by means of a continuous network model. Amazing facts in favor of this model are its astonishing simplicity and phenomenological success. It is much easier to handle than the Boltzmann transport equation, but is at least as successful as standard theory in accounting for phenomena such as the size effect of dc resistivity in thin films, bulk ac impedance in the microwave range, or absorption up to optical frequencies.

The impedance behavior of a metal which corresponds to the model is regular for any values of frequency or mean free electron path.

Our network applies to the one-dimensional case of transverse electric fields propagating at frequency ω through a half-space or plate of metal. It is the result of a

combined effort to represent mechanisms as electric analog circuits, and to compose from such circuitry, with mathematical and physical intuition, a phenomenologically realistic model. All physical quantities introduced with it are macroscopic quantities, e.g., the electric field or the current density in the metal at a particular position. Since the skin effect is a surface phenomenon, it is, however, natural to distinguish between two ensembles: the electrons moving towards the surface and those moving away from it. We developed the picture that an incident electric-field wave, as it propagates through the metal, excites in both ensembles current density waves which contain momentum and kinetic energy and get attenuated through friction with the lattice, and that the two ensembles act electrically on each other. Assuming then that the interactive fields provide coupling with an additional electromagnetic wave, the model could successfully be fitted to all known experimental evidence, but the interaction mechanism could not be interpreted physically.

Our network model demonstrates that anomalous current conduction in metals can be brought into a form which is handy and well suited for realistic computer simulation. We wish to point out especially that the network model generates an expression for the reciprocal surface impedance which fulfills the requirements of a response function in connection with the Kramers–Kronig equations and the sum rule.

In Part 2 the phenomenological qualities of the model will be exploited with the aim of developing a model for superconductors and discussing non-local electrodynamic properties of superconductors by means of the Kramers–Kronig and sum-rule equations.

2. Development and Discussion of the Conductivity Model

Let us consider a metal whose shape is either a half-space or an unbounded plate of thickness D, with surface(s) perpendicular to the x-axis of a Cartesian co-ordinate system, and located at the position(s) shown in Figures 1(a) and 1(b). Suppose that an external electric field of angular frequency ω is applied to the surface(s) in the y direction, so that electromagnetic fields $E = E_y(x, \omega)$ and $H = H_z(x, \omega)$ with associated current density $i = i_y(x, \omega)$ are set up in the metal, according to the Maxwell's equations

$$\frac{\partial E}{\partial x} = -j\omega\mu_0 H \tag{1}$$

$$-\frac{\partial H}{\partial x} = i + j\omega\varepsilon\varepsilon_0 E \tag{1'}$$

(μ_0 = magnetic vacuum permeability, ε_0 = dielectric vacuum permittivity, ε = dielectric constant of the metal.)

Equations (1) and (1') have a well-known analog representation; it is (in the absence of current i, which couples to additional network) the LC-transmission line for wave propagation plotted in Figure 2(a), with $L = \mu_0$, $C = \varepsilon\varepsilon_0$ as longitudinal and transverse line elements, with E as line voltage, H as line current and $i + j\omega\varepsilon\varepsilon_0 E$ (conduction plus displacement current density) as line-current change per unit length. The velocity of wave propagation defined by the LC line is the velocity of light $c = 1/\sqrt{LC} = 1/\sqrt{\mu_0\,\varepsilon\varepsilon_0}$ in the metal; the impedance is $z = \sqrt{L/C} = \sqrt{\mu_0/\varepsilon\varepsilon_0}$.

Now let us denote the current densities of the electron ensembles moving towards and away from the surface by i^- and i^+, and thus the current density in the metal by

$$i(x, \omega) = i^+(x, \omega) + i^-(x, \omega), \tag{2}$$

and let i^+ and i^- fulfill the transport equations

$$i^+ + \frac{l}{2(1+j\omega\tau)} \cdot \frac{\partial i^+}{\partial x} = \frac{E}{2\rho(1+j\omega\tau)} \tag{3}$$

$$i^- - \frac{l}{2(1+j\omega\tau)} \cdot \frac{\partial i^-}{\partial x} = \frac{E}{2\rho(1+j\omega\tau)}, \tag{3'}$$

where l, τ and ρ characterize material properties. Equations (2), (3) and (3') recall the familiar Boltzmann transport equation, and this stimulates the notations $\rho = \mathrm{dc}$

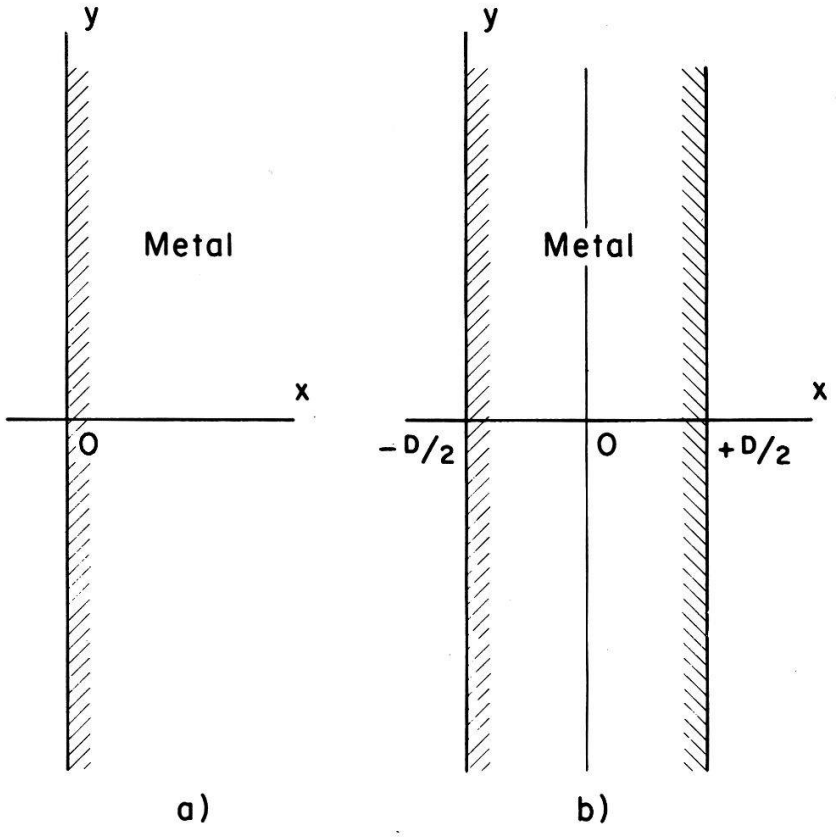

Figure 1
Reference of half-space (Fig. 1(a)) and plate (Fig. 1(b)) to a Cartesian coordinate system.

resistivity, $\tau =$ conduction-electron relaxation time, and $l =$ mean free path of the conduction electrons. There are, however, also deviations from the Boltzmann equation. We shall, therefore, work out the question of similarity or dissimilarity somewhat further and postpone notations for τ and l until their meaning has been discussed.

Standard theory starts from an electron distribution function in ordinary and velocity space $f(x, \vec{v}) = f_0(\vec{v}) + f_1(x, \vec{v})$, where f_0 denotes the undisturbed distribution function, and f_1 its distortion due to the applied field. f_1 is to be a solution of

$$f_1 + \frac{\tau \cdot v_x}{1+j\omega\tau} \cdot \frac{\partial f_1}{\partial x} = \frac{e \cdot \tau}{m(1+j\omega\tau)} \cdot \frac{\partial f_0}{\partial v_y} \cdot E \tag{4}$$

($e =$ electron charge, $m =$ electron mass) for stationary conditions. f determines the current density which reads

$$i = ne \int v_y \cdot f \cdot d^3 v \tag{5}$$

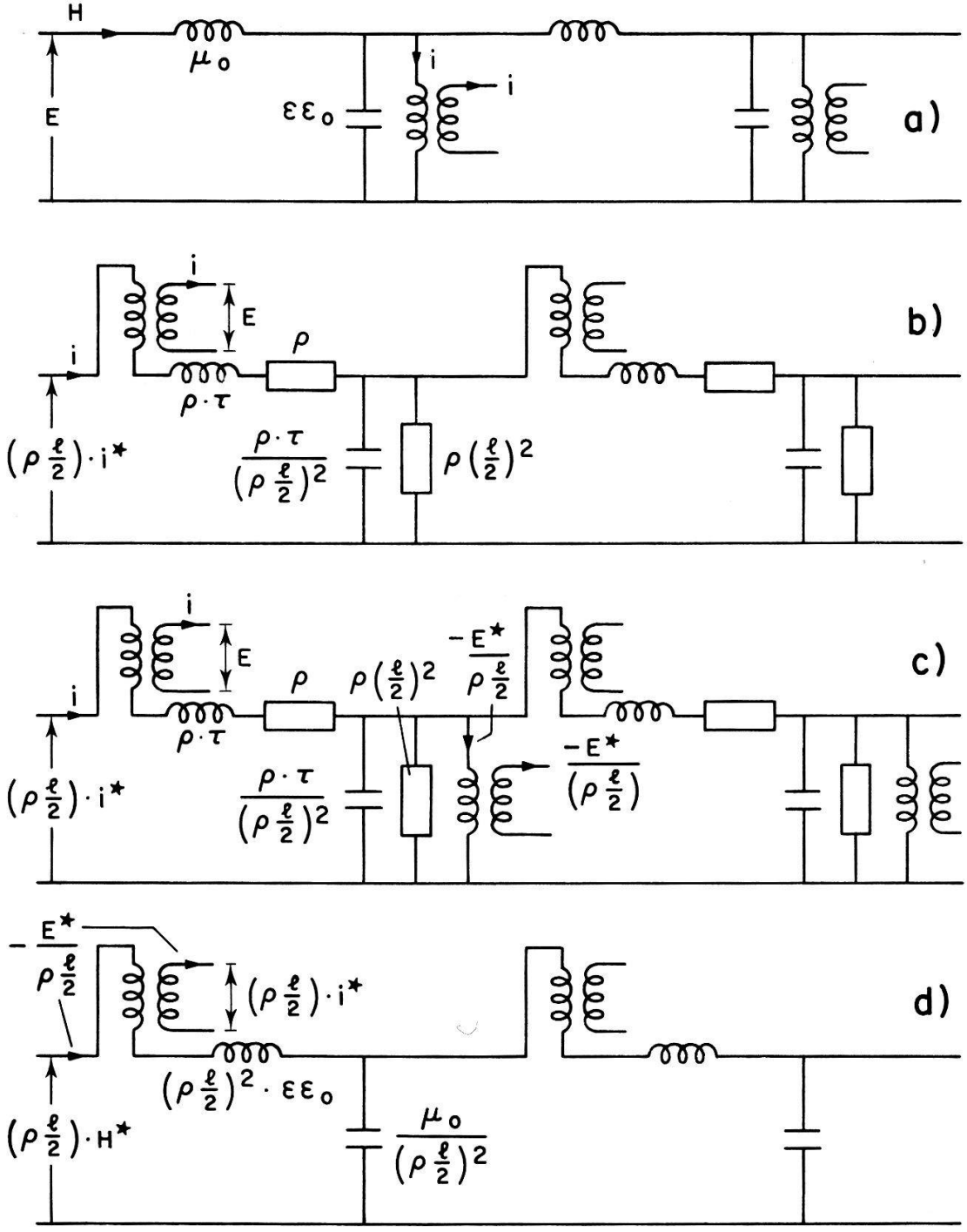

Figure 2
Analog model network.

(n = conduction-electron concentration). From the point of view of standard theory, equations (2), (3) and (3′) appear to yield approximate solutions in the sense that the conduction electrons are supposed (through *ad hoc* assumptions):

a) to behave like two collective groups, one containing all electrons moving in the forward, and the other containing all electrons moving in the backward x directions;

b) to assume velocities in the x direction whose absolute value is equal for all electrons and amounts to an average Fermi velocity $v_F/2$ for each group.

To convince ourselves, let us impose in equation (4) the condition $v_x = v_F/2$, multiply by $n \cdot e \cdot v_y/2$ and integrate in velocity space. We then find with equation (5) the momentum balance

$$i^+ + \frac{(v_F \cdot \tau)}{2(1 + j\omega\tau)} \cdot \frac{\partial i^+}{\partial x} = \frac{n \cdot e^2 \cdot \tau}{m(1 + j\omega\tau)} \cdot \frac{E}{2}, \tag{6}$$

which is exactly equation (3) if we identify $v_F \cdot \tau = l$ and $m/(n \cdot e^2 \cdot \tau) = \rho$. A completely analogous calculation yields equation (3′) for the backward-moving electron group.

Next we show that equations (3) and (3′) define a mechanism of current transport in terms of ordinary waves. For that purpose, let us introduce

$$i^* = i^+ - i^-, \tag{2′}$$

and transform equations (3) and (3′) by means of equations (2) and (2′) into

$$(\rho l/2) \cdot \frac{\partial i^*}{\partial x} = E - \rho(1 + j\omega\tau) \cdot i \tag{7}$$

$$(\rho l/2) \cdot \frac{\partial i}{\partial x} = -\rho(1 + j\omega\tau) \cdot i^*. \tag{7′}$$

Equations (7) and (7′) have the analog representation plotted in Figure 2(b); it is again an LC-transmission line for wave propagation, but with additional dissipative elements, and with facilities to couple into the Maxwellian transmission line of Figure 2(a). Line current and line voltage are i and $(\rho l/2) \cdot i^*$, respectively. The elements $L = \rho\tau$ and $C = \rho\tau/(\rho l/2)^2$ define for them a propagation velocity $v = 1/\sqrt{LC} = v_F/2$, and an impedance $z = \sqrt{L/C} = \rho l/2$. This property makes v_F and ρl fundamental parameters of the metal as in standard theory. The additional longitudinal and transverse dissipative elements, ρ and $\rho(l/2)^2$, respectively, cause damping at an attenuation length $l/2$. The total energy A stored on the L and C elements amounts to $A = \rho \cdot \tau \cdot (i^{*2} + i^2)/2$ per unit volume. If we recall equations (2) and (2′), write $i^+ = \text{nev}^+/2$, $i^- = nev^-/2$, and use $\rho = m/(n \cdot e^2 \cdot \tau)$, this energy transforms into $A = (n \cdot m/2) \cdot (v^{+2} + v^{-2})$, which is equal to the kinetic energy of n independent particles per unit volume.

We thus see that equations (2), (2′), (3) and (3′) build up a complete (although maybe unphysical) set which describes current transportation in terms of waves moving through a continuum. The waves are dampened due to friction with the lattice; in the absence of friction the wave motion is associated with just the energy density expected for free electrons. l is a measure for wave attenuation rather than a mean free path; τ measures the relaxation of current-density waves rather than of individual electrons. One has the choice of introducing either l or τ since $l = v_F \cdot \tau$.

A negative side of the model developed so far is that it fails to predict the well-established properties of the anomalous skin effect correctly.

It is not difficult to conceive intuitively why standard theory and the analog model become vastly different under conditions of anomalous current transport. According to Pippard [1] the anomalous current conduction arises from a selection process of the electrons contributing to the current due to shrinking penetration depth with increasing frequency. Only those electrons which move almost parallel to the metal surface and therefore spend almost their entire mean free path in the skin-depth region, contribute effectively to the current, while those moving perpendicularly to the favorite direction are most ineffective. In our model, such selection processes are excluded due to the assumption that all electrons move with $\pm v_F/2$ perpendicular to the surface.

Instead of rejecting, at this point, the concept of electron wave motion we investigated possibilities of obtaining agreement with experimental results by introducing an interactive electric field E^* between the forward and backward-moving electrons which provides coupling with an additional ordinary wave. In a first heuristic step we tried to set up such interaction by generalizing transport equations (3) and (3′) into

$$i^+ + \frac{l}{2(1+j\omega\tau)} \cdot \frac{\partial i^+}{\partial x} = \frac{E+E^*}{2\rho(1+j\omega\tau)} \tag{8}$$

$$i^- - \frac{l}{2(1+j\omega\tau)} \cdot \frac{\partial i^-}{\partial x} = \frac{E-E^*}{2\rho(1+j\omega\tau)}, \tag{8′}$$

by relating E^* to a magnetic field H^* through

$$\frac{\partial E^*}{\partial x} = j\omega\mu_0 H^*, \tag{9}$$

by relating (E^*, H^*) to the current density i^* through

$$\frac{\partial H^*}{\partial x} = i^* + j\omega\varepsilon\varepsilon_0 E^*, \tag{9′}$$

and finally by introducing (i, i^*) for (i^+, i^-) in equations (8) and (8′) by means of equations (2) and (2′); this yields, together with equations (1) and (1′), the set

$$\frac{\partial E}{\partial x} = -j\omega\mu_0 H \tag{10}$$

$$-\frac{\partial H}{\partial x} = i + j\omega\varepsilon\varepsilon_0 E, \tag{10′}$$

$$\frac{\partial E^*}{\partial x} = j\omega\mu_0 H^* \tag{11}$$

$$\frac{\partial H^*}{\partial x} = i^* + j\omega\varepsilon\varepsilon_0 E^*, \tag{11′}$$

$$(\rho l/2) \cdot \frac{\partial i^*}{\partial x} = E - \rho(1+j\omega\tau) \cdot i \tag{12}$$

$$(\rho l/2) \cdot \frac{\partial i}{\partial x} = E^* - \rho(1+j\omega\tau) \cdot i^* \tag{12′}$$

It turned out in a subsequent discussion of the analog properties of the set that it has remarkable qualities. To point this out, let us mention the following: Firstly, for equations (10) and (10′) the analog representation Figure 2(a) still applies; secondly, equations (12) and (12′) do not differ from equations (7) and (7′) except for the additional E^* term. We can account for this term by adding to the transmission line (Fig. 2(b)) which represents equations (7) and (7′) the coupling facilities shown in Figure 2(c); thirdly, equations (11) and (11′) meet with the analog representation plotted in Figure 2(d) which is an LC line with facilities to couple into the line Figure 2(c). Therefore, equations (10), (10′), (11), (11′), (12) and (12′) build a complete set which describes transport in terms of coupled ordinary waves.

In the added transmission line Figure 2(d), the line voltage is $(\rho l/2)\cdot H^*$, the line current $E^*/(\rho l/2)$. The elements $C = \mu_0/(\rho l/2)^2$ and $L = \varepsilon\varepsilon_0(\rho l/2)^2$ define a propagation velocity $c = 1/\sqrt{\varepsilon\varepsilon_0\mu_0}$ which is the velocity of light in the metal, and store reversibly the amount $(\varepsilon\varepsilon_0/2)\cdot E^{*2} + (\mu_0/2)\cdot H^{*2}$ of energy per unit volume. If the possibility is accepted that E^* and i^* point to the z direction and H^* to the y direction, then the wave represented by Figure 2(d) corresponds to an electromagnetic wave, with its plane of polarization perpendicular to that of the wave represented by Figure 2(a), and the amount of volume energy stored on the elements of line 2(d) is appropriate. This picture is certainly physically hypothetical, but as a matter of fact, it will turn out that we have been successful in developing a model with realistic phenomenological properties. We shall, subsequently, only demonstrate (Part 1) and exploit (Part 2) these phenomenological qualities, thus fortunately not depending on questions of physical interpretation.

It remains to introduce boundary conditions. While it is evident that at the metal surface(s) the electric field is equal to the applied field, the other conditions are less trivial. Reuter and Sondheimer [2] obtained the best agreement between theory and experiment when they supposed diffuse scattering of the individual electrons at the surface(s). We merely adapt their finding to diffuse scattering of the electron waves. This is achieved if we terminate the transmission line (Fig. 2(c)) with the matching impedance $\rho\cdot l/2$. Finally, we order vanishing flow $E^*\cdot H^*$ through the surface(s). This corresponds to $H^* = 0$, or short-circuiting the end(s) of the transmission line (Fig. 2(d)). In view of the boundary conditions imposed for H^*, and equation (11′), the current resulting from integrating the density $i^* + j\omega\varepsilon\varepsilon_0 E^*$ over the range of x values is zero.

Let us finally visualize the special case of the current-carrying plate (Fig. 1(b)) for dc conditions. Then, the current density i, which is constant deep in the metal, drops off symmetrically near the surfaces $x = \pm D/2$, but in these boundary zones, current density i^* is set up. i^* flows oppositely directed, but with equal strength, in the two surface layers, and so produces the magnetic field H^* spreading through the whole plate and becoming constant deep in the metal. If again the possibility is accepted that E^* and i^* are in the z direction and H^* in the y direction, then in a plate (or wire) the electron motion following straightly an applied electric dc field should be accompanied by 'screening' electron motion, confined to a surface layer, which produces a magnetic moment in the reversed direction of the applied electric field.

One may eliminate in equations (10) to (12′) all variables except one, and then find a differential equation of sixth order, but with even-order derivatives only. It is, therefore, in principle, possible to calculate solutions algebraically: solutions may be written as a sum of exponential functions $e^{\alpha x}$ with α a solution of the equation

$$\begin{cases} \sum_{k=0}^{3} A_{2k} \cdot \alpha^{2k} = 0, \\ \text{where} \\ A_0 = -\left[\left(\dfrac{j\mu_0\omega}{\rho\dfrac{l}{2}}\right)^2 - \dfrac{j2\mu_0^2\omega^3\varepsilon\varepsilon_0(1+j\omega\tau)}{\rho\left(\dfrac{l}{2}\right)^2} + \dfrac{(\varepsilon\varepsilon_0\mu_0\omega^2)^2(1+j\omega\tau)^2}{\left(\dfrac{l}{2}\right)^2}\right] \\ A_2 = \dfrac{j2\omega\mu_0(1+j\omega\tau)}{\rho\left(\dfrac{l}{2}\right)^2} - \dfrac{2(1+j\omega\tau)^2\varepsilon\varepsilon_0\mu_0\omega^2}{\left(\dfrac{l}{2}\right)^2} + (\varepsilon\varepsilon_0\mu_0)^2\omega^4 \\ A_4 = -\left[\left(\dfrac{1+j\omega\tau}{\dfrac{l}{2}}\right) - 2\varepsilon\varepsilon_0\mu_0\omega^2\right]^2 \\ A_6 = 1. \end{cases} \tag{13}$$

In the following section, we shall compare the solutions of equation (13) with experimental experience.

3. Results

3.1. Dc effects: the size effect of thin-film resistivity

For $\omega = 0$, equation (13) simplifies into

$$\alpha^2 - \frac{1}{(l/2)^2} = 0. \tag{14}$$

The current density in a film which is an unbounded plate of thickness D placed in a co-ordinate system as shown in Figure 1(b) calculates easily to

$$i(x) = \frac{E}{\rho}\left[1 - e^{-D/l} \cdot \cosh\left(\frac{2x}{l}\right)\right], \tag{15}$$

and the ratio of film resistivity, ρ_F, to bulk resistivity, ρ, becomes

$$\frac{\rho_F}{\rho} = \frac{1}{1 - \dfrac{l}{2D}\left[1 - e^{-2D/l}\right]}. \tag{16}$$

$\log\rho_F/\rho$ versus $\log 2D/l$ is plotted in Figure 4 (solid line).

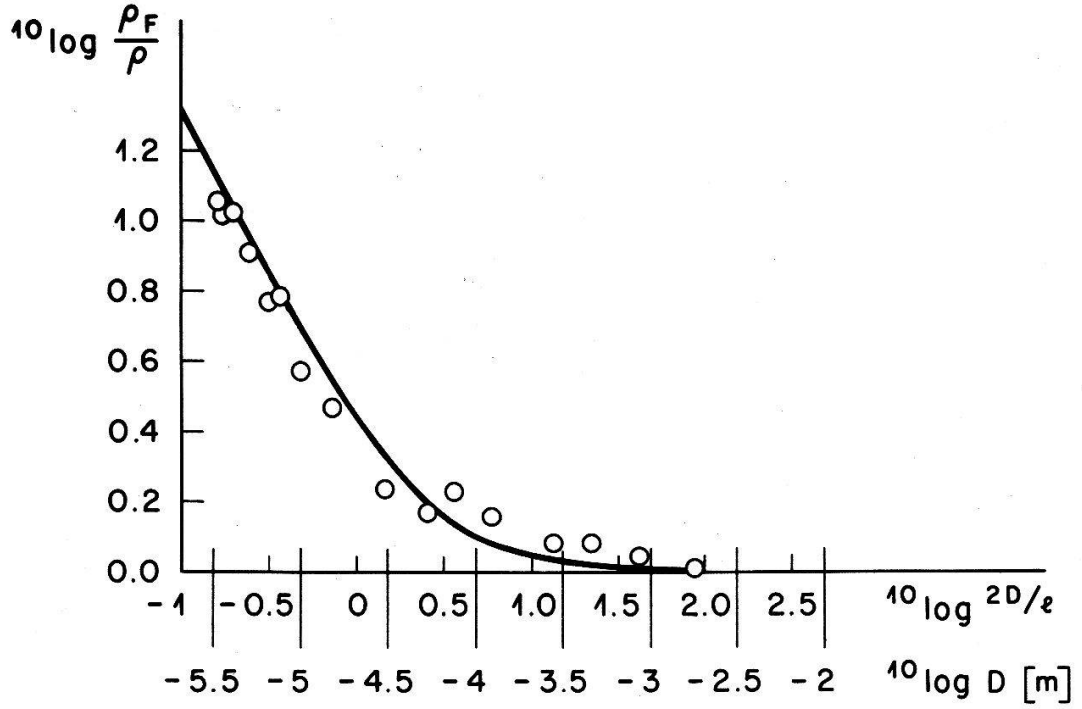

Figure 3
Size effect of thin-film resistivity: Data by Andrew [6] (circles) fitted to theoretical curve (full line). ρ_F = film resistivity, ρ = bulk resistivity, D = film thickness, $l/2$ = electron-wave attenuation length.

If the resistivity of films with various thicknesses is measured at the same temperature, the results may be fitted into this plot to find the best value of $l/2$, and from this, ρl. There is no room for adjustments then for $l/2$, which is certainly a positive aspect of this evaluation procedure for ρl, but unfortunately, due to considerable experimental

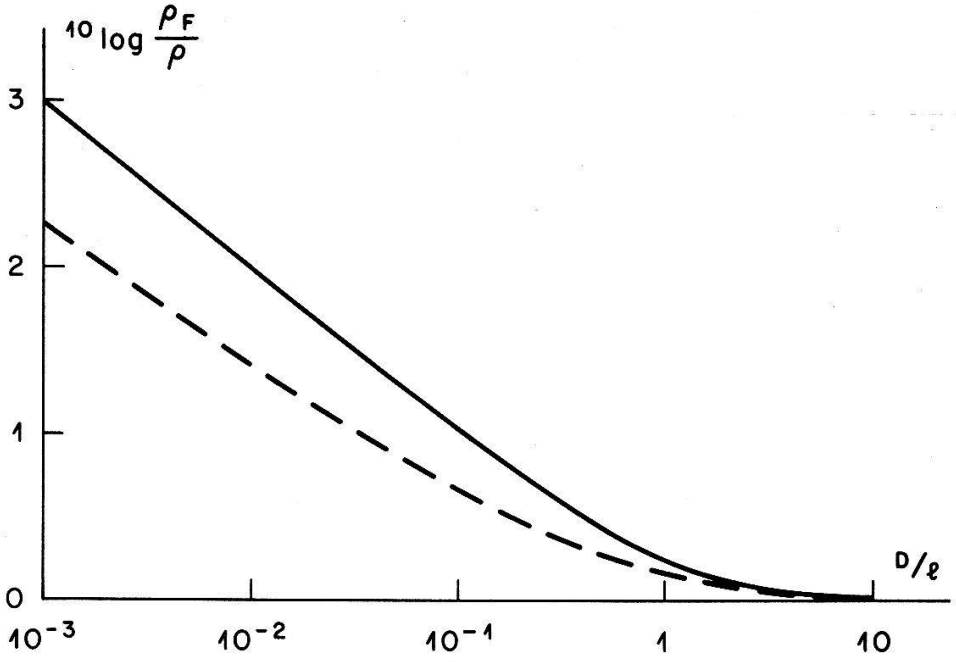

Figure 4
Size effect of thin-film resistivity: Comparison between present theory (full line) and Reuter–Sondheimer theory (broken line). ρ_F = film resistivity, ρ = bulk resistivity, D = film thickness, $l/2$ = electron-wave attenuation length (l = mean free path).

difficulties with thin-film preparation and uncertainty about surface scattering, investigations on the size effect are often of limited credibility, or incomplete. As an example, we have carried out the fitting procedure with the data of Andrew [5] for tin at 3.8°K (circles in Fig. 3), and find $l/2 = 2.1 \cdot 10^{-5}$ m and (with $\rho = 11.5 \cdot 10^{-8}\ \Omega \cdot$m at room temperature and a residual resistance ratio $r = 1.78 \cdot 10^{-4}$) $\rho l = 8.6 \cdot 10^{-16}\ \Omega \cdot \text{m}^2$. Andrew's data have been analyzed in the frame of standard electron theory by Sondheimer [6]. He finds a larger $\rho l = 2.0 \cdot 10^{-15}\ \Omega \cdot \text{m}^2$, however, in disagreement with $\rho l = 9.5 \cdot 10^{-16}\ \Omega \cdot \text{m}^2$ determined in the same frame from bulk-material ac effects, which he believes to yield more reliable results with carefully prepared specimens. More recent measurements by Kunzler and Renton [7] provide increased confidence in the experimental situation involved with the size effect, but confirm that standard free-electron theory leads to different values for ρl when dc or ac effects are evaluated; dc values are roughly twice as high as ac values. Our model yields a tendency towards smaller ρl values from evaluation of the size effect. This immediately becomes evident from inspection of Figure 4, where we have simultaneously plotted ρ_F/ρ as a function of D/l according to equation (16) (full line) and according to the Reuter–Sondheimer theory (broken line).

3.2. *Ac effects*

3.2.1. The surface impedance of bulk material in the microwave region. The microwave impedance $z = R + jX$ of a metal has been analyzed experimentally at frequencies $\omega/2\pi = 1.2 \cdot 10^9$ and $\omega/2\pi = 3.6 \cdot 10^9$ cycles/sec for a variety of metals by Pippard and Chambers [8, 9]. The experimental method used to measure the surface resistivity, R, involves construction of a resonator of the metal to be studied, and determination of its selectivity Q; for a given resonator, Q is proportional to $1/R$. Q is measured as a function of temperature, and plotted against σ, the dc conductivity of the metal. Such plots can be scaled to fit theoretical curves of the Reuter–Sondheimer theory in which A/R is computed against $\alpha^{1/6} \cdot (A = (6^{1/6} \cdot (\rho l \cdot (\omega \mu_0)^2)^{1/3})/2;\ \alpha = 3/4 \cdot (\mu_0 \omega l^2/\rho))$. The agreement is almost exact, as shown in Figures 5(a) and 5(b). It is then possible, by reading off the values of α corresponding to any pair of values of R and σ, to estimate ρl for any metal; $\rho l = \sqrt{\frac{4}{3} \cdot (\alpha/\mu_0 \omega \sigma^3)}$. We have computed for the frequencies $\omega/2\pi = 1.2 \cdot 10^9$ and $\omega/2\pi = 3.6 \cdot 10^9$ cycles/sec the shape of A/R against $\alpha^{1/6}$ according to the set of equations (10) to (12′), and scaled the curves to fit those of the Reuter–Sondheimer theory. The result is plotted in Figure 6(a). Both theoretical curves are apparently very similar, although not quite identical. Figure 6(b) shows plots of reciprocal surface reactance, $1/X$, against $\alpha^{1/6}$ for both theories; again the curves deviate only slightly. In the limiting case of extreme departure ($\alpha \gg 1$) from classical conditions ($\alpha \ll 1$), the surface impedance Z_∞ was calculated algebraically. We found

$$Z_\infty = \frac{1}{2 \cdot 2^{1/3}} \cdot (\mu_0 \cdot \omega)^{2/3} \cdot (\rho l)^{1/3} \cdot (1 + j\sqrt{3}) \tag{17}$$

and thus confirm the predictions of standard electron theory that Z_∞ varies as $\omega^{2/3}$ and is independent of l, and that $[X/R]_\infty = \sqrt{3}$.

3.2.2. Bulk absorption in the optical region. At the microwave frequencies considered so far, $\omega \cdot \tau$ has always been small compared with unity. But for sufficiently high frequencies $\omega \cdot \tau \gg 1$; the terms arising from the displacement current may become appreciable, and eventually even dominant. A classical metal $[\rho(\omega) = \rho(0) \cdot (1 + j\omega\tau)]$ behaves as shown in Figure 7 (broken line): its absorptivity as a function of frequency (expressed in corresponding (vacuum) light wavelengths) varies as $\sqrt{\omega}$ at low frequencies (this is the Hagen–Rubens relation), is then constant over a wide range of intermediate frequencies, but increases steeply towards one when the plasma frequency

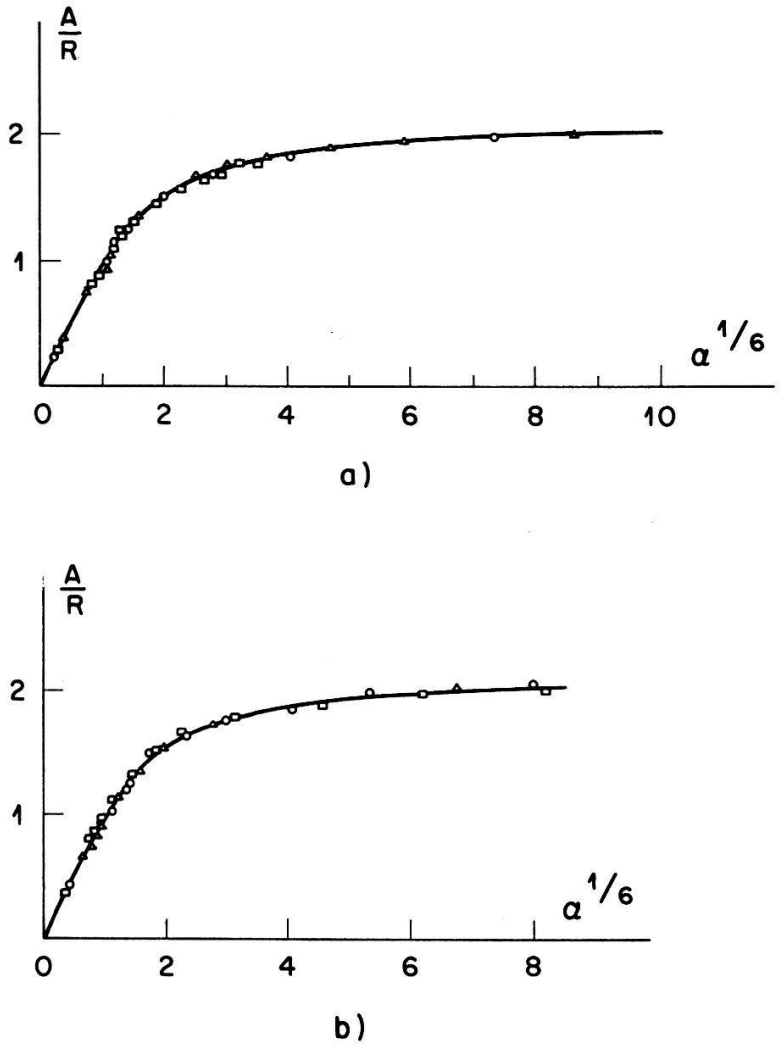

Figure 5
(a) Experimental results on the surface resistance R as a function of temperature (dc conductivity) fitted to theoretical plots of A/R against $\alpha^{1/6}$ (see text for definition of A and α). $\omega = 2\pi \cdot 1.2 \cdot 10^9$ cycles/sec; □ = copper, △ = silver, ○ = tin. (b) $\omega = 2\pi \cdot 3.6 \cdot 10^9$ cycles/sec; □ = gold, △ = lead, ○ = silver. After Sondheimer [7] and Chambers [10].

$\omega_P = 1\sqrt{\varepsilon \cdot \varepsilon \cdot \rho \cdot \tau}$ is reached; then the metal is transparent to light with a higher frequency than ω_P. The plot in Figure 7 refers to a conductivity $\sigma = 4.1 \cdot 10^9\ \Omega^{-1} \cdot m^{-1}$, and a dielectric constant $\varepsilon = 1$.

The absorptivity of real metals deviates considerably from this theory at low temperatures, but only little quantitative information is available, due to experimental difficulties with sample preparation and mainly measuring techniques. Fortunately,

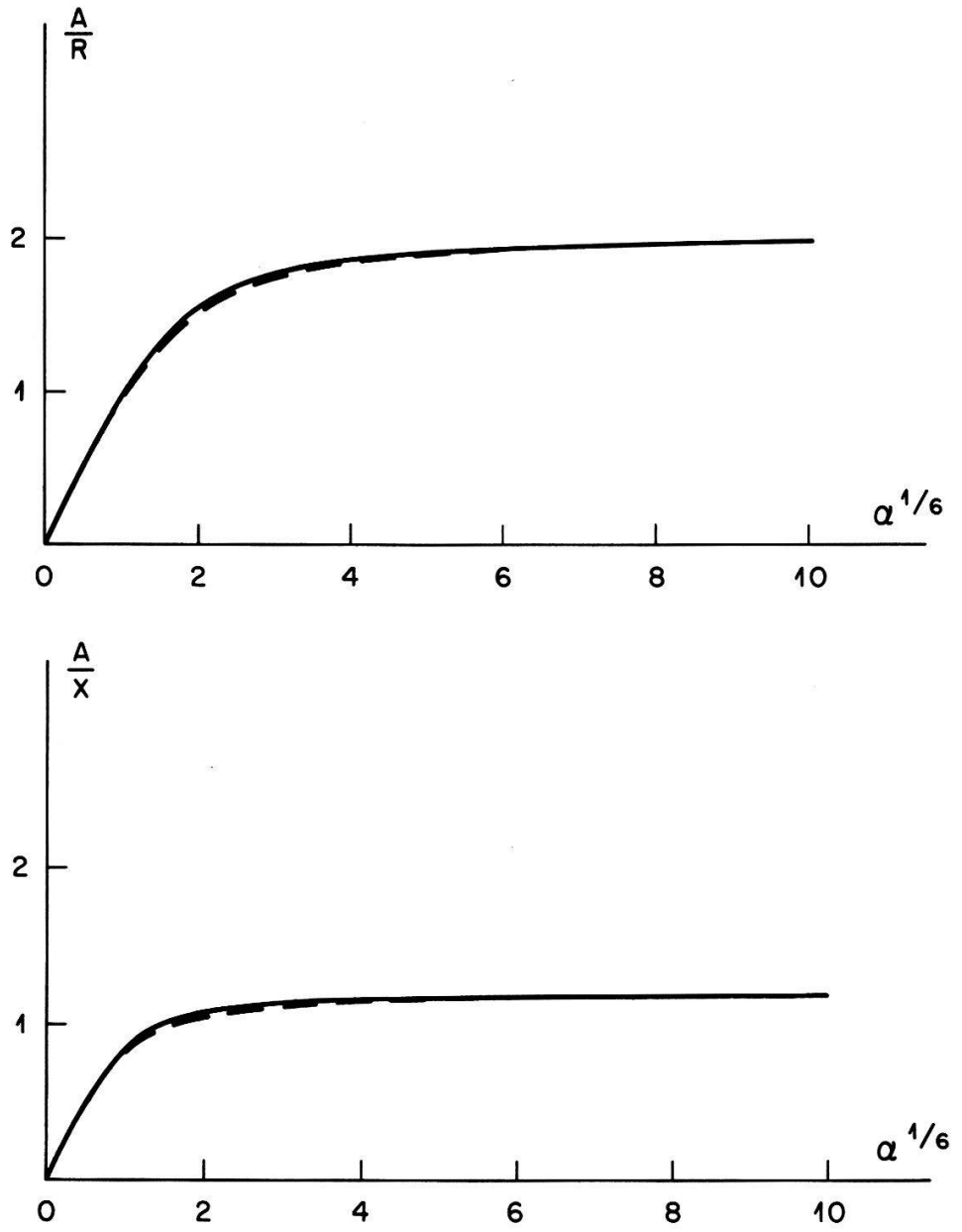

Figure 6
Theoretical dependence of surface impedance $R + jX$ on temperature: Comparison of plots A/R (Fig. 6(a)) and A/X (Fig. 6(b)) against $\alpha^{1/6}$ according to present theory (full line) and Reuter–Sondheimer theory (broken line). See text for definition of A and α.

data for copper[1]) at 4.2°K with $\sigma = 4.1 \cdot 10^9 \cdot \Omega^{-1} \cdot m^{-1}$ have been determined by Biondi [10][2]) in the most attractive wavelength range $0.3 < \lambda < 3.5$ micron. These are plotted in Figure 7 (full line connecting circular points) and show the region of constant absorptivity at a much higher threshold level $A = 50 \cdot 10^{-3}$ ($^{10}\log A = -2.30$) and the high-pass filter cutoff at a much larger wavelength $\lambda \sim 0.5$ micron.

Theoretical absorption curves computed by Sondheimer [6] and Dingle [11] demonstrate that standard electron theory qualitatively accounts for the high level of absorptivity, provided that diffuse surface scattering of the conduction electrons is

[1]) And silver.

[2]) $\sigma = 4.1 \cdot 10^9\ \Omega^{-1} \cdot m^{-1}$ follows from $\sigma = ne^2\tau/m^*$ with $n = 8.5 \cdot 10^{28}\ m^{-3}$, $m^*/m = 1.38$, $T \cdot \tau = 1.0 \cdot 10^{-11}$ sec·°K.

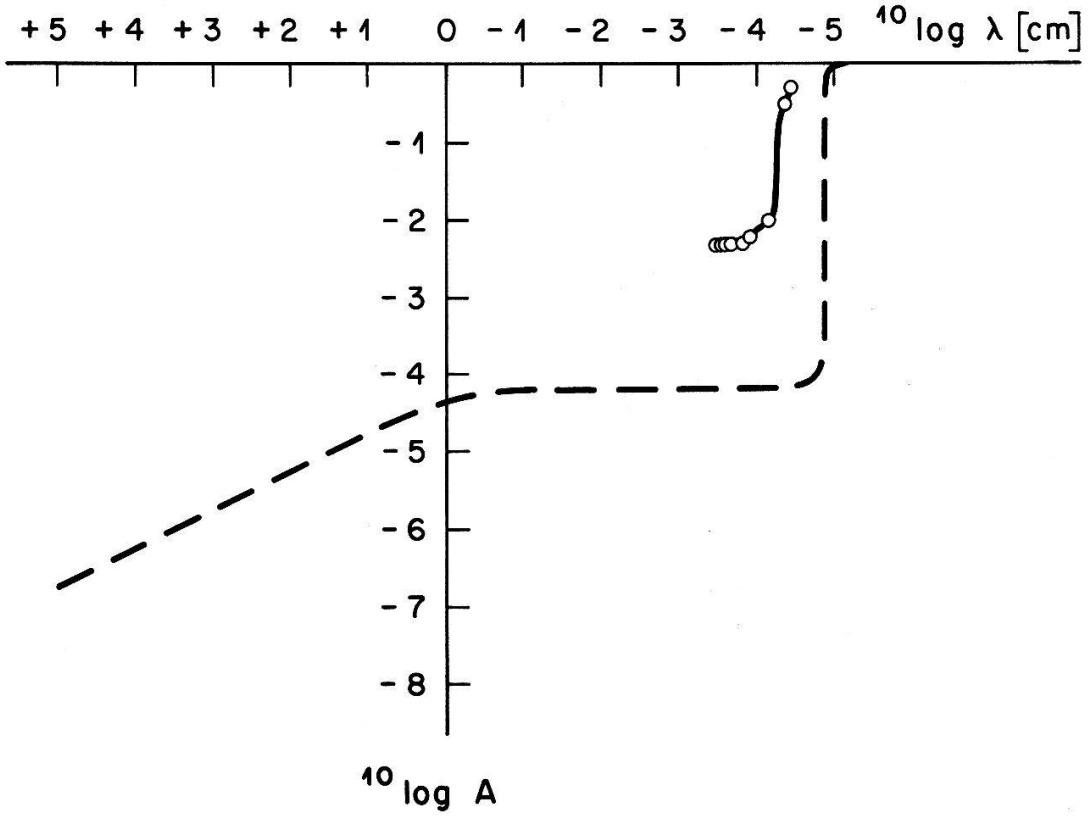

Figure 7
Absorption coefficient A of copper as a function of frequency (expressed in corresponding light vacuum wavelengths, λ). Experimental (circles between full line) after Biondi [11], theoretical (broken line) according to $\sigma = \sigma_0 \cdot (1 + j\omega\tau)$ with data $\sigma_0 = 4.1 \cdot 10^9\ \Omega^{-1} \cdot m^{-1}$ and $\tau = 2.4 \cdot 10^{-12}$ sec after Biondi [11].

assumed, but physical parameters are almost invisibly hidden behind extended numerical computations.

Theoretical curves of the absorption coefficient

$$A = \frac{4 \cdot R \cdot \sqrt{\frac{\mu_0}{\varepsilon_0}}}{\left(R + \sqrt{\frac{\mu_0}{\varepsilon_0}}\right)^2 + X^2} \tag{18}$$

against frequency (or corresponding wavelength of light) calculated with our equations (10) to (12′) reveal, at intermediate frequencies, a threshold whose level depends directly on the Fermi velocity, and a cutoff frequency which depends directly on the dielectric constant[3]). Plots referring to copper ($\rho l = 6.49 \cdot 10^{-16}\ \Omega \cdot m^2$ evaluated from microwave impedance measurements) with $\sigma = 4.1 \cdot 10^9\ \Omega^{-1} \cdot m^{-1}$ are shown in Figures 8(a) and 8(b). We thus dispose of a simple procedure to scale these material parameters. Biondi's data on copper fit to theoretical absorption curves for $v_F = 1.48 \cdot 10^6$ m/sec and $\varepsilon \approx 16$. The value of v_F is almost equal to $v_F = 1.56 \cdot 10^6$ m/sec of standard free-electron theory, and the value of ε is in the range of values measured in semiconductors.

[3]) This is not different from standard theory.

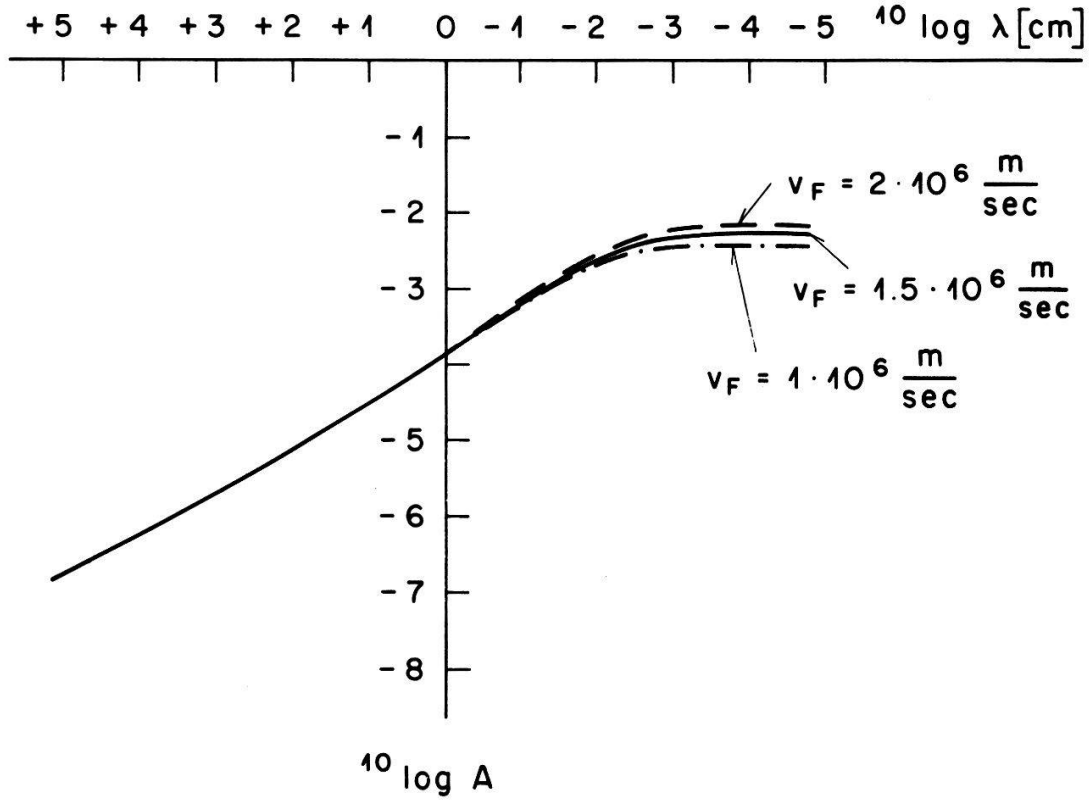

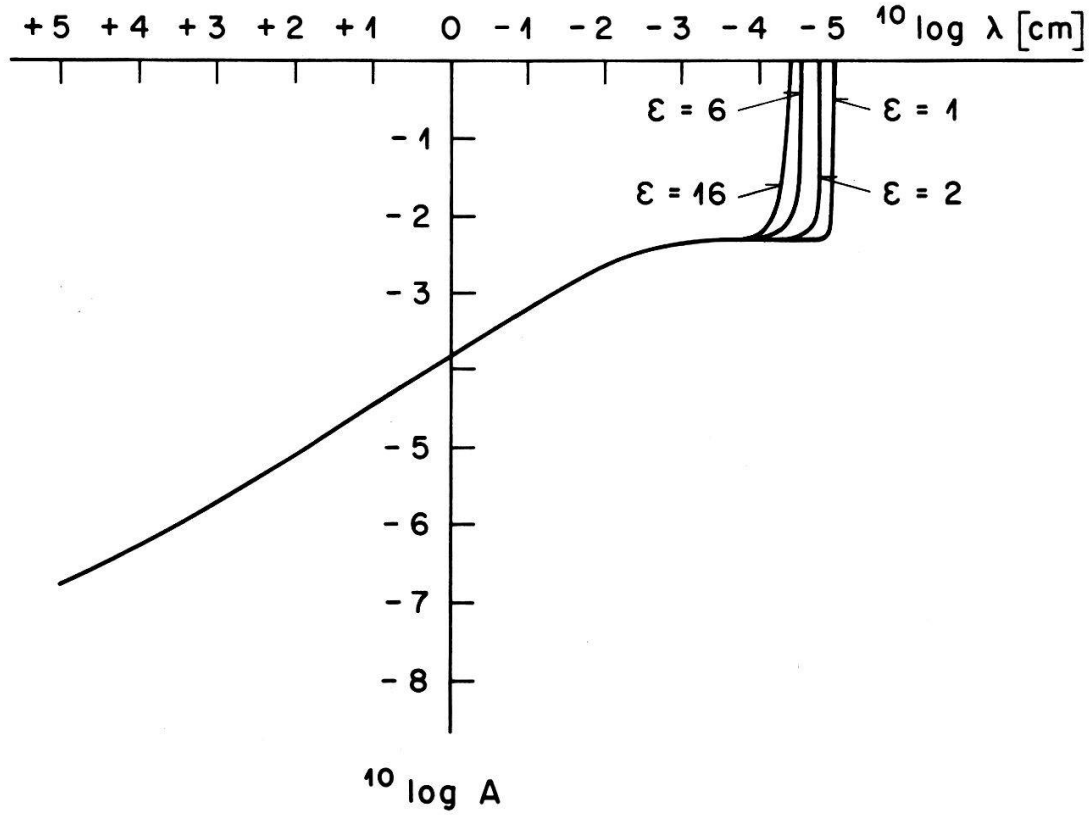

Figure 8
Absorption coefficient A of copper as a function of frequency (expressed in corresponding light wavelengths, λ), with v_F (Fig. 8(a)) or ε (Fig. 8(b)) as a parameter, according to present theory with data $\rho l = 6.49 \cdot 10^{-16}\ \Omega \cdot m^2$, $\sigma_0 = 4.1 \cdot 10^9\ \Omega^{-1} \cdot m^{-1}$.

3.2.3. The shape of a penetrating electric field. It is common to the Reuter–Sondheimer theory and ours that the shape of a penetrating electric field is exponential in the classical region, but that a 'tail' of small amplitude penetrates under extreme anomalous skin-effect conditions to a much larger distance below the surface. The tails are, however, strongly contrasting, if one looks at them more closely. Sondheimer [6] finds a tail

$$E(x/l) \sim c_1 \cdot e^{-s_1 \cdot (x/l)} + c_2 \cdot e^{-(x/l)}/(x/l)^2 \tag{19}$$

for $x \gg l$ where c_1 and c_2 are constants, and where s_1 is a complex parameter whose real part increases steadily with $\alpha = \frac{3}{4}(\mu_0 \omega/\rho) l^2$. Unity is reached when $\alpha = \alpha_0 = 2.63$.

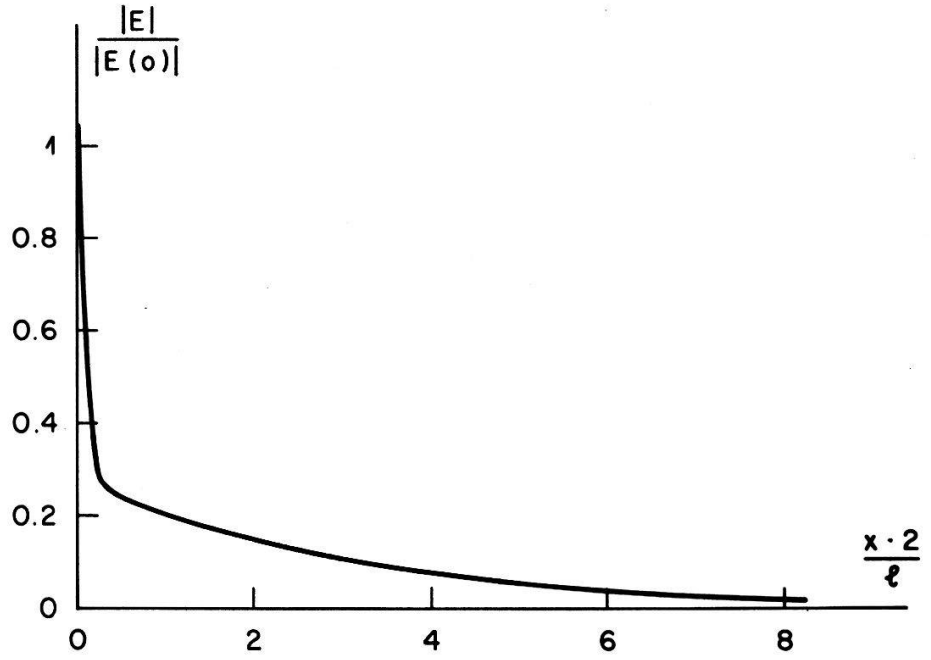

Figure 9
Electric-field amplitude $|E|$ as a function of distance x from the surface of a half-space. $|E(0)| = 1$; $l/2$ = electron-wave attenuation length.

The first term in equation (19) is 'regular' in the sense that the field in the metal, at sufficient distances from the surface, appears unaffected by the presence of the surface. The second term is 'irregular' in the sense that field excitation is conditioned by the presence of the surface even deep in the metal. The irregular term dominates for $\alpha \gg \alpha_0$. Then the electric field, though largely confined to the surface, has a tail of effective length l, which may be regarded as being transmitted into the metal by electrons which move in the interior under the influence of no forces except their collisions with the lattice.

In our case $E(x)$ is always regular; electron motion in the small amplitude tail which builds up for $\alpha \gg 1$ is strongly supported by the interaction forces between electron waves. An example of field penetration into a half-space is plotted in Figure 9. The curve is for a frequency $\omega = 2\pi \cdot 3.6 \cdot 10^9$ cycles/sec; further data are those previously used for copper ($\rho l = 6.49 \cdot 10^{-16}\ \Omega \cdot m^2$, $\sigma = 4.1 \cdot 10^9\ \Omega^{-1} \cdot m^{-1}$, $v_F = 1.48 \cdot 10^6\ m \cdot sec^{-1}$), thus $\alpha = 618.5$ ($\alpha^{1/6} = 2.92$).

4. Outlook

In Part 2, we shall first make use of the similarity between the electromagnetic properties of normal conductors and superconductors to set up an analog model for the pure superconducting (low-frequency) state, and introduce an approximate model for all frequencies. Kramers–Kronig relations and sum rule are then exploited to relate individual parameters of the models of Parts 1 and 2. This technique, already used earlier by Tinkham and Ferrell [12], but under less specified conditions, permits in our frame a quantitative analysis; we shall further recognize limitations of linear methods which are set up by nonlinearity associated with a two-fluid model of superconductivity.

References

[1] A. B. Pippard, Proc. Roy. Soc. (London) A, *191*, 385 (1947).
[2] G. E. H. Reuter and E. H. Sondheimer, Proc. Roy. Soc. (London) A, *195*, 336 (1948).
[3] A. B. Pippard, G. E. H. Reuter and E. H. Sondheimer, Phys. Rev. *73*, 920 (1948).
[4] B. Serin, Phys. Rev. *72*, 1261 (1947).
[5] E. R. Andrew, Proc. Phys. Soc. (London) A, *62*, 77 (1949).
[6] E. H. Sondheimer, Phil. Mag. *1*, 1 (1952).
[7] J. E. Kunzler and C. A. Renton, Phys. Rev. *108*, 1397 (1957).
[8] R. G. Chambers, Nature, *165*, 239 (1950); or see Sondheimer [6].
[9] R. G. Chambers, Proc. Roy. Soc. (London) *215*, 481 (1952).
[10] M. Biondi, Phys. Rev. *102*, 964 (1956).
[11] R. B. Dingle, Physica *19*, 311 (1953).
[12] M. Tinkham and R. A. Ferrell, Phys. Rev. Letters *8*, 331 (1959).